

The Mid-Fusiform Sulcus (*sulcus sagittalis gyri fusiformis*)

KEVIN S. WEINER *

¹Department of Psychology, UC Berkeley, Berkeley, California

²Helen Wills Neuroscience Institute, Berkeley, California

ABSTRACT

In the human brain, the mid-fusiform sulcus (MFS; *sulcus sagittalis gyri fusiformis*) divides the fusiform gyrus (FG) into lateral and medial partitions. Recent studies show that the MFS is identifiable in every hemisphere and is a landmark that identifies (a) cytoarchitectonic transitions among four areas of the FG, (b) functional transitions in many large-scale maps, and (c) the location of fine-scale functional regions. Thus, simply identifying the MFS in a person's brain provides researchers with knowledge regarding: (a) how cells are organized across layers within a particular cortical location, (b) how functional representations will be laid out in cortex, and (c) the precise location of functional regions from cortical folding alone. The predictive power of the MFS can guide future studies examining the anatomical-functional organization of the FG, as well as the development of translational applications for different patient populations. Nevertheless, progress has been slow in incorporating the MFS into the broader anatomical community and into neuroanatomical reference sources. For example, even though the MFS is a rare structural-functional landmark in human association cortex as just described, it is not recognized in the recently published *Terminologia Neuroanatomica (TNA)*. In this review, I collate the anatomical and functional details of the MFS in one place for the first time. Together, this article serves as a comprehensive reference regarding the anatomical and functional details of the MFS, as well as provides a growing number of reasons to include the MFS as a recognized neuroanatomical structure in future revisions of the *TNA*. *Anat Rec*, 302:1491–1503, 2019. © 2018 American Association for Anatomy

Key words: fusiform gyrus; neuroanatomy; occipital lobe; temporal lobe; visual cortex

INTRODUCTION

Located in ventral occipito-temporal cortex of the hominoid brain, the fusiform gyrus (FG) performs functionally specialized computations underlying face perception (Kanwisher et al., 1997; Puce et al., 1996, 1999; Nobre et al., 1998; Rossion et al., 2003; Grill-Spector et al., 2004; Rossion, 2008; Parvizi et al., 2012; Grill-Spector and Weiner, 2014; Rangarajan et al., 2014), object recognition (Malach et al.,

1995; Gauthier et al., 1999; Gauthier et al., 2000; Grill-Spector 2003; Konen et al., 2011; Gauthier and Tarr, 2016), and reading (Cohen et al., 2000; Wandell et al., 2012; Glezer and Riesenhuber, 2013; Bouhali et al., 2014). A longitudinal sulcus known as the mid-fusiform sulcus (MFS) divides the FG into lateral and medial partitions (Puce et al., 1996; Nobre et al., 1998; Allison et al., 1999; Weiner and Grill-Spector 2010; Nasr et al., 2011; Weiner et al., 2014). Though the MFS was defined and labeled as the *sulcus sagittalis gyri*

Grant sponsor: University of California, Berkeley.

*Correspondence to: Kevin S. Weiner, Department of Psychology, 2121 Berkeley Way West, UC Berkeley, Berkeley CA 94720. E-mail: kweiner@berkeley.edu

Received 27 April 2018; Revised 28 August 2018; Accepted 11 September 2018.

DOI: 10.1002/ar.24041
Published online 24 November 2018 in Wiley Online Library (wileyonlinelibrary.com).

fusiformis in 1896 by Retzius (1896), it was mentioned only a handful of times in papers and atlases for the next 100 years until it re-appeared in the cognitive neuroscience literature in 1996 (Weiner and Zilles, 2016 for review). Within the last decade, a plethora of studies have shown that the MFS identifies (a) cytoarchitectonic transitions among four areas of the FG (Caspers et al., 2013; Weiner et al., 2014; Lorenz et al., 2017; Weiner et al., 2017a; Rosenke et al., 2018), (b) functional transitions in many large-scale functional maps (Weiner et al., 2014; Weiner et al., 2010; Nasr et al., 2011; Grill-Spector and Weiner, 2014; van den Hurk et al., 2015; Jacques et al., 2016; Kadipasaoglu et al., 2016), and (c) the location of fine-scale functional regions (Weiner and Grill-Spector 2010; McGugin et al., 2014; Weiner et al., 2014, 2017a; McGugin et al., 2015; Jacques et al., 2016; Kadipasaoglu et al., 2016) that are causally implicated in visual perception (Parvizi et al., 2012; Rangarajan et al., 2014). Together, the findings from these studies have established the MFS as an anatomical and functional landmark in the human brain.

Nevertheless, progress has been slow in incorporating the MFS into the broader anatomical community and into neuroanatomical reference sources because most—if not all—of the findings summarized in the previous paragraph are published in neuroimaging and cognitive neuroscience journals. As such, even though the MFS is identifiable in every human brain to the point in which an algorithmic approach can be implemented to automatically identify the MFS on cortical surface reconstructions (Weiner et al., 2018), it is not recognized in the recently published *Terminologia Neuroanatomica* (TNA; FIPAT, 2017; Ten Donkelaar et al., 2017, 2018). Consequently, the main goal of the present work is to provide a comprehensive review of these empirical findings regarding the MFS, which can serve as a reference source for the extended anatomical and cognitive neuroscience fields moving forward.

To achieve this goal, this review can be divided into eight sections. First, I review recent findings revealing that the MFS displays morphological features that are identifiable from childhood to adulthood, as well as are identifiable in living and post-mortem brains. The second section reviews a series of recent studies that identified cytoarchitectonic transitions among four areas within the MFS using observer-independent methods: one in the posterior FG between areas FG1 and FG2 (Caspers et al., 2013; Weiner et al., 2014), as well as one in the middle portion of the FG between areas FG3 and FG4 (Lorenz et al., 2017). The third section shows that these cytoarchitectonic transitions correspond well with transitions in large-scale functional maps in which the cortical expanse lateral to the MFS is functionally distinct from the cortical expanse medial to the MFS. The fourth section further details that while the entire MFS identifies functional transitions in large-scale maps, particular features of the MFS identify the location of fine-scale functional regions. The fifth section discusses recent findings showing that the endpoints of white matter fascicles terminate in

predictable locations relative to the MFS. The sixth section expands on how knowledge of the MFS opens new questions about the evolution of ventral occipito-temporal cortex in hominoids. The seventh section discusses how identifying and measuring different anatomical and functional features of the MFS has translational applications that have clinical and functional significance in different patient populations. Finally, the eighth section situates the MFS within nearby gyri and sulci presently accepted by the TNA (FIPAT, 2017; Ten Donkelaar et al., 2017, 2018). Together, this article serves as a comprehensive reference source regarding the anatomical and functional details of the MFS, as well as provides a growing number of reasons to include the MFS as a recognized neuroanatomical structure in future revisions of the TNA.

The MFS is Identifiable in Every Brain with Morphological Features that are Identifiable from Childhood to Adulthood, As Well As in Living and Post-Mortem Brains

The MFS is a longitudinal sulcus within the FG that divides the FG into lateral and medial partitions (Retzius 1896; Bailey and von Bonin, 1951; Puce et al., 1996; Nobre et al., 1998; Allison et al., 1999; Weiner and Grill-Spector, 2010, 2013; Nasr et al., 2011; Petrides, 2012; Grill-Spector and Weiner, 2014; McGugin et al., 2014; Weiner et al., 2014; Yeatman et al., 2014; McGugin et al., 2015; van den Hurk et al., 2015; Gomez et al., 2015; Lorenz et al., 2017; Jacques et al., 2016; Kadipasaoglu et al., 2016; Natu et al., 2016; Weiner and Zilles, 2016; Gomez et al., 2017; Weiner et al., 2017a). This macroscopic definition of the MFS has been consistent since the first identification of the *sulcus sagittalis gyri fusiformis* by Retzius (1896). Specifically, a translation of Retzius' original description reads:

“It is known, that the inferior surface of the temporal lobe is concave in anterior–posterior direction; this is particularly true for the Fusiform Gyrus. A sagittal sulcus along the midline can be very frequently found on its surface, which might be called *Sulcus sagittalis gyri fusiformis*. This sulcus can be uninterrupted and visible for a long distance, but is often subdivided into two or more parts, which may have branches and join neighboring sulci, which leads to a complicated pattern of the gyrus; if, however the Sulcus sagittalis is clearly visible and well developed, the surface of the gyrus can be subdivided into two parallel, sagittal convolutions, the Gyrus medius and lateralis, which are found separated in some cases or connected by bridges in other cases. These gyri can be followed far posterior, where they extend over the edge of the hemisphere and merge with the convolution of the occipital lobe, inferior temporal gyrus, and lingual gyrus in one or the other way”. P. 142¹

¹ Translation from Karl Zilles, which can be found in Weiner and Zilles, 2016. The original excerpt in German reads: “Die untere Fläche des Temporallappens ist bekanntlich von vorn nach hinten ausgehöhlt; dies gilt ganz besonders von dem Gyrus fusiformis. An dieser ihrer Fläche lässt sich sehr oft längs der Mittellinie eine sagittale Furche, die *Sulcus sagittalis gyri fusiformis* heissen mag, nachweisen. Diese Furche kann zuweilen einheitlich und eine weite Strecke verfolgbar sein, doch ist sie öfter in zwei oder mehrere Furchenstücke zerklüftet, welche auch verästelt und mit

den Nachbarfurchen vereinigt sein können, wodurch das Furchenbild der Windung compliciert wird; wenn aber der Sulcus sagittalis rein und stark ausgeprägt ist, zerfällt ihre Oberfläche in zwei parallele, sagittale Windungen, die *Gyrus medius und lateralis*, welche, bald ohne Verbindung, bald durch Brücken vereinigt, weit nach hinten verfolgbar sind, bis über die Mantelkante hinaus treten und in der einen oder anderen Weise mit den Windungen des Occipitallappens, dem Gyrus temporalis inferior und dem Gyrus lingualis, Verbindungen eingehen”. P. 142.

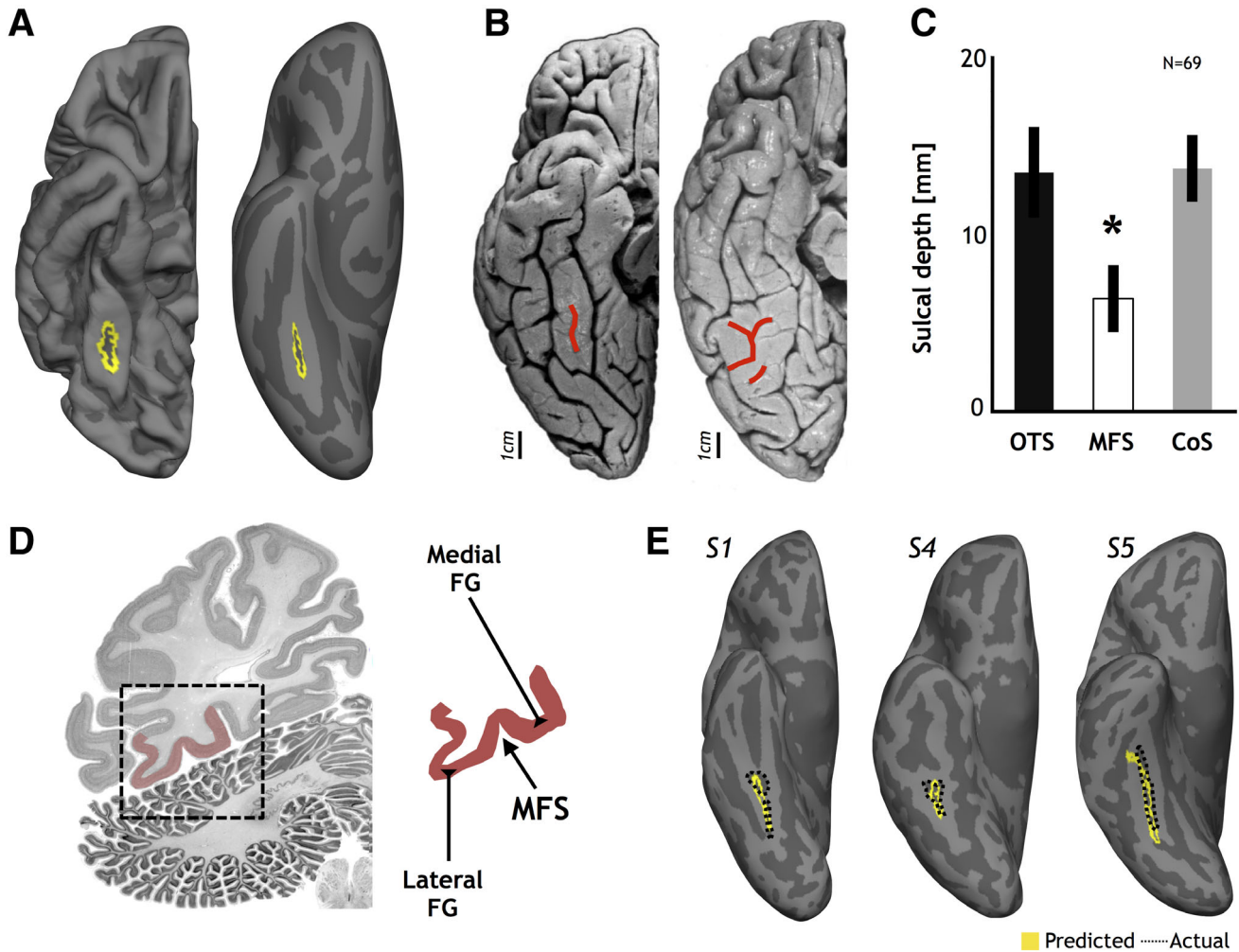


Fig. 1. The identification and morphology of the mid-fusiform sulcus. (A) A cortical surface reconstruction of the right hemisphere (ventral view) from the FreeSurfer software package ($N = 39$; freesurfer.net). The MFS is outlined in yellow. Left: wrinkled. Right: inflated. (B) Photographs of two right hemispheres from post-mortem individuals. The MFS is indicated in red. Left: 79-year-old female (image adapted from Lorenz et al., 2017). Right: 75-year-old male (image adapted from Weiner and Zilles 2016). (C) Sulcal depth measurements of the OTS, MFS, and CoS averaged across 69 living participants. Each bar (\pm std) represents data averaged across hemispheres and subjects. The MFS is significantly more shallow than either the OTS or CoS, $*P < 10^{-38}$. Specifically, the CoS and OTS are more than twice as deep as the MFS, which was also replicated in post-mortem brains (adapted from Weiner et al., 2014). (D) An example cell body stained coronal histological section. The difference in depth among the MFS, OTS, and CoS generates a distinctive pattern in single slices despite morphological differences on the cortical surface. The medial and lateral FG are easily discriminable based on the location of the MFS (modified from Weiner and Zilles, 2016). (E) The MFS can be automatically identified based on predictions from average cortical surfaces. Specifically, using cortex-based alignment tools, the MFS from (A) can be projected to individual subjects. Irrespective of morphological differences discussed in the text, the predicted MFS (yellow) aligns well with the actual MFS (dotted) in individual hemispheres (modified from Weiner et al., 2018). The MFS label file on the FreeSurfer average cortical surface can be downloaded here: <https://www.github.com/VPNL/MFS>. CoS: collateral sulcus; FG: fusiform gyrus; MFS: mid-fusiform sulcus; OTS: occipito-temporal sulcus.

After Retzius' observation, the MFS was mentioned (with different names) only a handful of times within the literature and in reference atlases for the next five decades (Mickle, 1897; Vogt 1904; Connolly, 1950; Bailey and von Bonin, 1951) until reappearing in the cognitive neuroscience literature 100 years after his original observation (Puce et al., 1996; Nobre et al., 1998; Allison et al., 1999; see Weiner and Zilles, 2016 for an extensive review).

Once the MFS re-surfaced in the literature in the late 1990s, it would almost be another 20 years before the stable and variable morphological features of the MFS would be assessed (Weiner et al., 2014). In terms of stability, the MFS was (a) identifiable in all 158 hemispheres

included in that study, which included both living and post-mortem brains from individuals spanning in age from 7 to 85, and (b) consistently about half as deep compared to the OTS and CoS (Weiner et al., 2014). The difference in depth between the MFS and surrounding sulci generates a distinctive pattern on single coronal slices of the brain—whether within *in vivo* T1 images or post-mortem histological sections (Fig. 1).

In contrast to the stable shallowness of the MFS, the MFS can vary significantly in terms of its length—ranging from 2.0 mm to 56.3 mm (Nasr et al., 2011; Weiner et al., 2014). The difference in length affects the location of the posterior, not the anterior, tip of the MFS.

Specifically, the anterior tip of the MFS aligns with the posterior tip of the hippocampus (Grill-Spector and Weiner, 2014). The MFS also varies in fractionation and intersection with the OTS and CoS. From previous analyses, in nearly half (48.55%) of the hemispheres examined, the MFS appears as a single longitudinal sulcus independent of the OTS and CoS in both children and adults (Weiner et al., 2014; Fig. 1). In the rest of the hemispheres examined (51.45%), the MFS varies in terms of its fractionation, as well as its intersection with the OTS and CoS. These stable and variable features are equally as likely to appear in (a) a child's brain or an adult's brain and (b) in a living brain or a post-mortem brain. Importantly, it does not take the expert eyes of trained anatomists to identify the MFS. Algorithmic approaches that leverage cortex-based alignment among individuals (Dale et al., 1999; Fischl et al., 1999) automatically identify the MFS and accurately discriminate it from surrounding sulci (Fig. 1).

Taken together, the macroscopic description of the MFS has not changed between Retzius' original observations and present quantifications. In particular, Retzius described the MFS as a sulcus dividing the FG into medial and lateral partitions, which is how present neuroanatomists and cognitive neuroscientists also define the MFS. Additionally, the first morphological analyses of the MFS revealed that (a) the MFS is identifiable in every brain, (b) its most stable morphological feature is its shallowness, (c) its most variable feature is its length, and (d) despite the variable features, the stable features among individual hemispheres enable the MFS to be defined automatically using tools that leverage cortex-based alignment.

The MFS is a Cytoarchitectonic and Receptor Architectonic Landmark

Classic cytoarchitectonic studies of the human brain commonly concluded that sulci seldom served as landmarks of cytoarchitectonic transitions outside of primary sensory cortices (Smith, 1907; Brodmann, 1909; Economo and Koskinas, 1925; Bailey and von Bonin, 1951). However, a main limitation of those classic studies is that neuroanatomists were manually examining histological tissue under a microscope and deciding, in an observer-dependent fashion, when one part of the tissue was cytoarchitectonically dissociable from an adjacent piece of tissue. Over the last few decades, a major methodological advancement occurred when researchers treated cytoarchitectonic analyses as an image processing problem. That is, instead of manually examining the tissue under a microscope, automated algorithms were devised to traverse the cortical ribbon and to determine if and where adjacent pieces of tissue were cytoarchitectonically different from one another (Zilles, 1978; Zilles et al., 1978; Zilles et al., 1980; Wree et al., 1982; Istomin and Shklyarov, 1984; Schleicher et al., 1986; Serra, 1986; Zilles et al., 1986; Rauch et al., 1989; Schleicher and Zilles, 1990; Schleicher and Zilles, 1990; Ahrens et al., 1990; Istomin and Amunts, 1992; Amunts et al., 1995; Schlaug et al., 1995; Schleicher et al., 1999; Schleicher et al., 2005; Amunts and Zilles, 2015). Using these methods, four areas have been parcellated in the human FG (Figs. 2 and 3). In the posterior FG, FG1 is located on the medial FG and extends into the CoS, while FG2 is located on the lateral FG and extends into the OTS

(Caspers et al., 2013). Moving more anteriorly to the middle portion of the FG, FG3 is located on the medial FG and extends into the CoS, while FG4 is located on the lateral FG and extends into the OTS (Lorenz et al., 2017).

In both the posterior and middle FG, the algorithmic approach identified cytoarchitectonic transitions within the MFS (Weiner et al., 2014; Lorenz et al., 2017). This is worth emphasizing because the algorithmic cytoarchitectonic approach identifies cytoarchitectonic boundaries independent of cortical folding. Thus, if the algorithm identifies the boundary at a particular cortical location that is reproducible between hemispheres in the same person and brains from multiple participants, then it is meaningful and serves as a landmark. In the posterior FG, the MFS identifies a cytoarchitectonic transition between FG1 and FG2 (Weiner et al., 2014). FG1 displays a columnar arrangement of small pyramidal cells and a thin and cell sparse layer IV (Caspers et al., 2013). FG2 shows large pyramidal cells in layer III, a prominent layer IV, but a less pronounced columnar organization. Additionally, FG2 is characterized by a higher cell density compared to FG1 (Caspers et al., 2013; Figs. 3 and 4). In the middle portion of the FG, the MFS also identifies a cytoarchitectonic transition between FG3 and FG4 (Lorenz et al., 2017). FG3 shows a compact and dense layer II, a prominent sub-layer IIIc with medium-sized pyramidal cells, and little clusters of granular cells in layer IV (Lorenz et al., 2017). FG4 has a less densely packed layer II, broad layer III, a thin, moderately dense layer IV, and a cell dense layer VI (Lorenz et al., 2017). Concomitantly, the MFS is a landmark identifying cytoarchitectonic transitions among four areas within the posterior and middle portions of the FG.

Since these FG areas have only been parcellated within the last 5 years, a useful exercise is to compare their cortical location to the classic cytoarchitectonic parcellations within the FG. This is possible because classic cytoarchitectonic areas of the human brain have been aligned to the FreeSurfer average cortical surface. For instance, Brodmann's parcellation (defined in the PALS-B12 atlas by Van Essen, 2005) and the Economo and Koskinas (1925) parcellation (manually delineated by Scholtens et al., 2018) have both been aligned to the FreeSurfer average surface. Consequently, qualitative comparisons can be made among the areas of the classic, observer-dependent parcellations and those of the modern, observer-independent parcellations within the FG. In comparison to Brodmann's scheme, FG areas 1–4 from the observer-independent scheme overlap with Area 37. Additionally, FG1 and FG2 overlap with Area 19, while FG3 and FG4 overlap with Area 20. In comparison to the scheme of Economo and Koskinas (1925), FG1 and FG2 are largely contained within Area PH, while FG3 and FG4 are largely contained within area TF. Interestingly, if we consider (a) FG1 and FG2 as a posterior cluster and (b) FG3 and FG4 as an anterior cluster, the observer-dependent TF/PH boundary resembles the observer-independent boundary differentiating the FG1/FG2 posterior cluster from the FG3/FG4 anterior cluster (Fig. 4A), especially in the left hemisphere at the group level.

As a final point in this section, it is worth emphasizing that the MFS not only identifies cytoarchitectonic transitions, but also differences in receptor density across cortical layers (known as receptor architecture) in the posterior FG (Caspers et al., 2015a, b; Fig. 4B). As transmitter

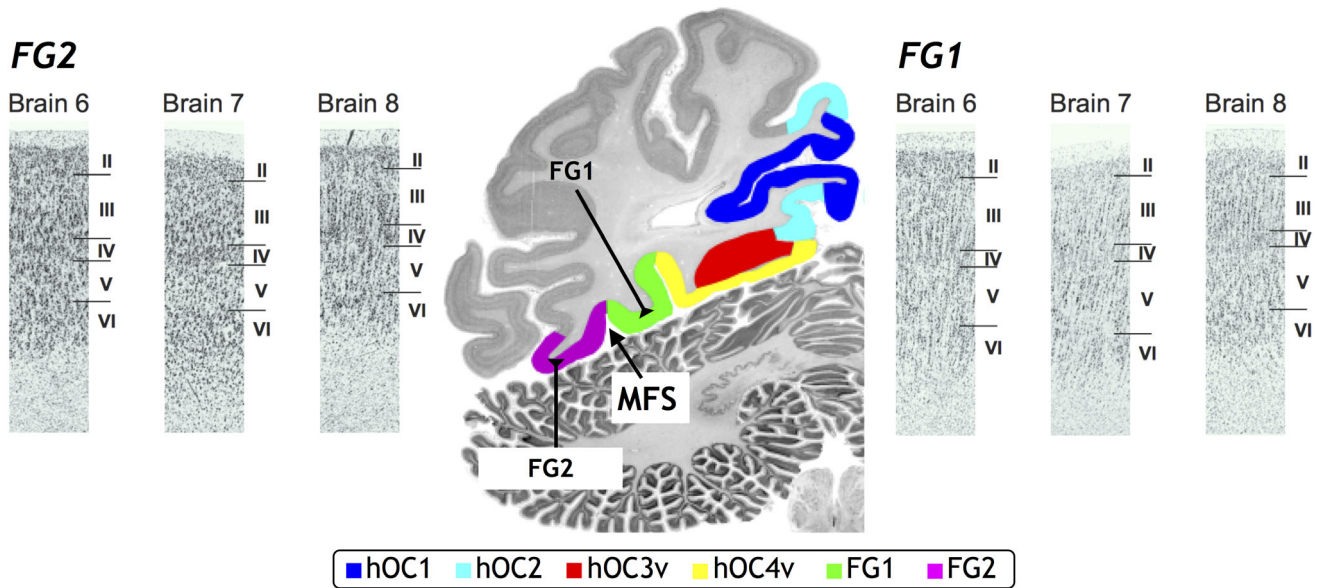


Fig. 2. The cytoarchitecture of the posterior MFS. Middle: Using observer-independent methods (Amunts and Zilles, 2015 for review), cytoarchitectonic areas can be defined using an algorithmic and statistical approach. Six areas within visual cortex are shown (see legend). This observer-independent approach identified a cytoarchitectonic transition between FG1 (green) and FG2 (magenta) in the MFS. To anchor the reader, this is the same histological section in Figure 1D. Right: Example histological sections of FG1 from three different brains. Roman numerals indicate cortical layers. Left: Same, but for FG2. Note that despite the fact that the slices are from different brains and there is inter-individual variability, the main cytoarchitectonic differences identified by the algorithm are: (1) FG1 is more columnar than FG2 and (2) FG2 has a greater cell density than FG1. Images adapted from Caspers et al., 2013. FG1-4: fusiform gyrus areas 1–4.

receptors are key molecules of neurotransmission, differences in receptor architecture reflect differences in functional architecture. Figure 4B illustrates the relationship among the algorithmic cytoarchitectonic delineation of FG1 and FG2, the MFS, and the laminar distribution of 5-HT_{1A} receptors along the cortical ribbon (Caspers, 2013; Caspers et al., 2015a, b). Quantifying the densities of different receptor binding sites across cortical layers within areas FG1 and FG2 empirically showed that these areas differ in the densities of 5-HT_{1A}, NMDA, GABA_A, GABA_B, M₃, and nicotinic α 4/ β 2 receptors. Thus, knowing the location of the MFS also predicts differences in receptor density across cortical layers in the posterior FG, which has functional implications for interpreting cellular architecture (Fig. 4B, right).

Together, these findings across studies indicate that the MFS is a rare landmark identifying microarchitectonic transitions in human association cortex. These findings boast an impressive amount of predictive power: cellular insight can be gleaned from a macroanatomical location on the cortical surface.

The MFS is a Landmark Identifying Transitions in Many, Large-Scale Functional Maps

Over the last several decades, neuroimaging studies have identified many large-scale functional gradients, or maps, in human ventral occipito-temporal cortex. Interestingly, each of these maps contains a similar functional topology: neural responses on the lateral FG extending into the OTS are functionally distinct from neural responses on the medial FG extending into the CoS. For example, preferential neural responses for processing

visual stimuli presented in the center of the visual field (known as a foveal bias) are located on the lateral FG and OTS, while preferential neural responses for processing visual stimuli presented in the peripheral portion of the visual field (known as a peripheral bias) are located on the medial FG and CoS. This orderly representation of functional responses on the cortical sheet is known as an *eccentricity bias* map (Fig. 5A; Malach et al., 2002). Intriguingly, the functional transition in this map is predicted by the MFS. Specifically, in children, adolescents, and adults (ranging in age from 7 to 40), the functional transition in this map occurs 4.1–4.6 mm from the fundus of the MFS. Though that was the only study to explicitly quantify the functional transition in a large-scale map relative to the MFS, a recent review article (Grill-Spector and Weiner, 2014) showed that the MFS qualitatively identified the functional boundary in additional functional maps containing representations of animacy (Haxby et al., 2011), real world object size (Konkle and Oliva, 2012), semantics (Huth et al., 2012), domain selectivity (Nasr et al., 2011), and conceptual knowledge (Martin, 2007). Importantly, this organization generalizes across multiple types of neuroimaging techniques. For example, while the measurements just described were conducted with functional magnetic resonance imaging (fMRI), these functional transitions have also been identified with invasive measurements in patient populations using electrocorticography (Jacques et al., 2016; Kadipasaoglu et al., 2016) or intracranial depth electrodes (Jonas et al., 2016; Rossion et al., 2018).

It should also be stated that though the MFS is a crucial landmark in visual cortex, being able to see is not a pre-requisite for the MFS to be a functional landmark.

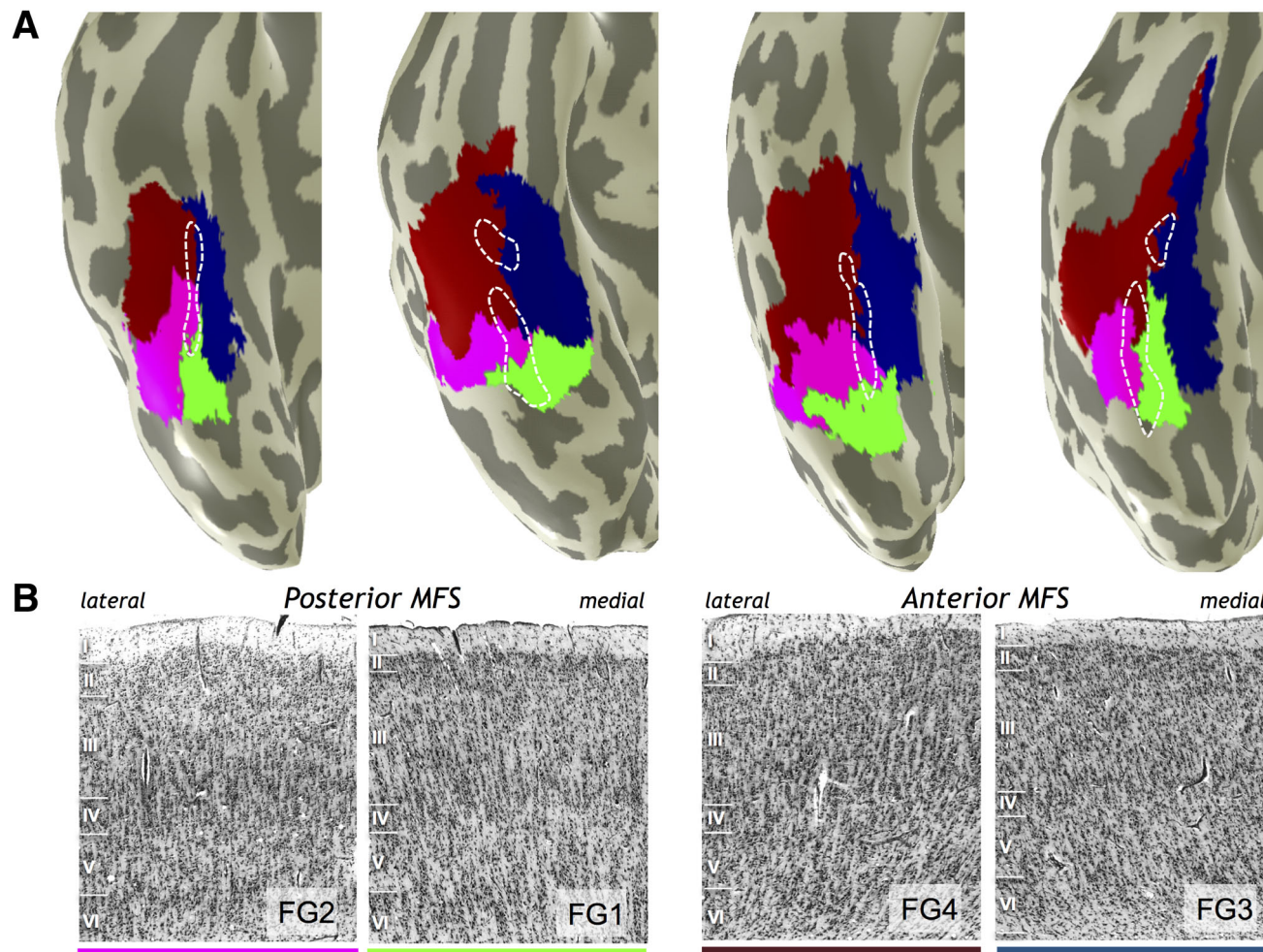


Fig. 3. The cytoarchitecture of the MFS. (A) Cytoarchitectonic areas FG1 (green), FG2 (magenta), FG3 (blue), and FG4 (maroon) projected to the inflated cortical surface of right hemispheres from four individuals. The border between FG1 and FG2 occurs within the posterior MFS (dotted line), whereas the border between FG3 and FG4 occurs within the anterior MFS. Because borders were defined using a quantitative, observer-independent algorithm that is independent of cortical folding, it is meaningful that the boundary among the FG areas occurs reliably within the MFS across hemispheres in the same brain, as well as across participants. Modified from Lorenz et al., 2015. (B) Each panel depicts an example histological slice of a cytoarchitectonic area (all sections are taken from the same brain). Note differences in the packing density of cells, the size and shape of cell bodies, and the width of cortical layers, which together form the basis to distinguish cytoarchitectonic areas from one another. Roman numerals indicate cortical layer. Modified from Rosenke et al., 2018. FG1-4: fusiform gyrus areas 1-4; MFS: mid-fusiform sulcus.

Indeed, the MFS also identifies functional representations in blind individuals (van den Hurk et al., 2015). Similar to the ending of the previous section, these findings also boast an impressive amount of predictive power: simply identifying the MFS in a person's brain predicts how functional representations will be laid out in cortex and additionally, where distinctions, or boundaries, of functional representations will occur.

The Anterior Tip of the MFS is a Landmark Identifying the Location of a Fine-Scale Functional Region Selective for Images of Faces

The FG has long been associated with visual perception. For example, neuropsychological case studies reveal that damage to the FG results in different types of perceptual disorders such as object agnosia and prosopagnosia (Damasio et al., 1982; Farah, 1990; Rossion, 2008;

Konen et al., 2011). Additionally, since the early 1990s, neuroimaging studies have identified regions that are face-selective (e.g., selective in the sense that neural responses are higher to images of faces compared to neural responses to images of non-face categories) on the FG (Sergent et al., 1992; Haxby et al., 1994; Puce et al., 1995; Kanwisher et al., 1997). Within the last decade, improved neuroimaging methods and data analyses within individual subjects noted that face-selective regions have a tight correspondence with cortical folding (Weiner and Grill-Spector, 2010; Weiner et al., 2010, 2014; Nasr et al., 2011). Specifically, the MFS serves as a landmark identifying face-selective regions on both a lateral-medial axis, as well as an anterior-posterior axis. On a lateral-medial axis, the MFS reliably discriminates face-selective regions on the lateral FG from place-selective regions within the CoS (Weiner and Grill-Spector, 2010; Weiner et al., 2010, 2014; Nasr et al., 2011). On an anterior-posterior axis,

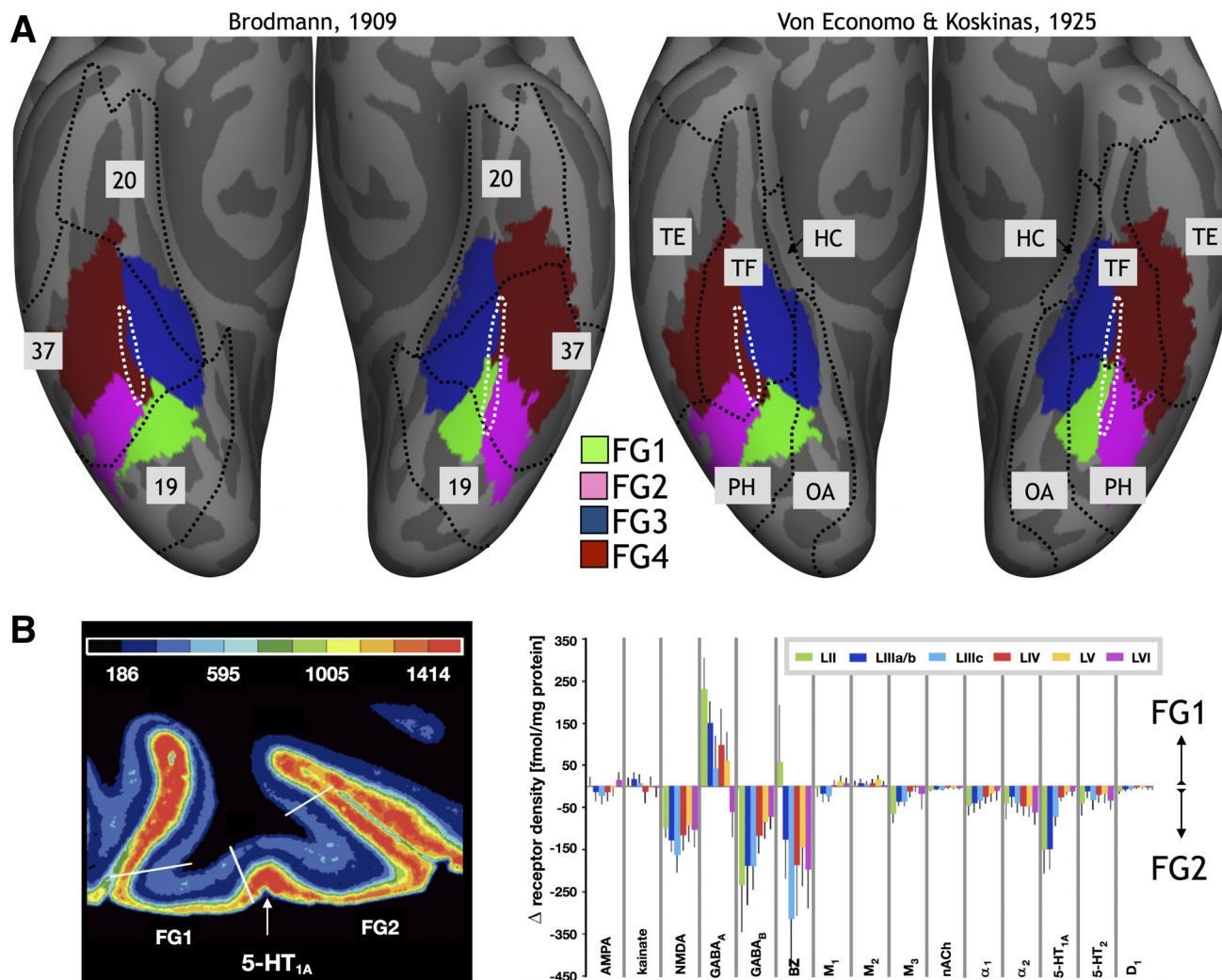


Fig. 4. Situating microanatomical understanding of the MFS relative to other classic and present cellular measurements. (A) Two widely cited cytoarchitectonic parcellations of the 20th century are those produced by Brodmann (1909; left), as well as the later parcellation of Economo and Koskinas (1925) (right). Approximations for both parcellations have been aligned to the FreeSurfer average surface and thus, can be qualitatively compared to the observer-independent parcellations of FG1-4. Compared to Brodmann's scheme, FG areas 1-4 from the observer-independent scheme overlap with his Area 37. Additionally, FG1 and FG2 overlap with his Area 19, while FG3 and FG4 overlap with his Area 20. Compared to Von Economo and Koskinas' scheme, FG1 and FG2 are largely contained within their Area PH, while FG3 and FG4 are largely contained within their area TF. Interestingly, the observer-dependent TF/PH boundary is near the observer-independent boundary differentiating the FG1/FG2 posterior cluster from the FG3/FG4 anterior cluster. (B) Left: Color coded autoradiograph in which colors indicate receptor concentration. The receptors measured in this example slice were 5HT_{1A}. White lines: boundaries of cytoarchitectonic areas FG1 and FG2. Arrow indicates MFS. Modified from Caspers, 2013. Right: A summary of the change in receptor density as a function of receptor type and cortical layer (see legend). Any bars in the lower half of the plot indicate higher densities in FG2 compared to FG1 and vice versa. Thus, knowing the location of the MFS also predicts differences in receptor density across cortical layers in the posterior FG. FG1-4: fusiform gyrus areas 1-4; MFS: mid-fusiform sulcus. Modified from Caspers et al. (2015).

the MFS accurately discriminates the location of face-selective regions from one another. In fact, building a 1 cm disk at the anterior tip of the MFS defines $83 \pm 7\%$ of mFus-faces/FFA-2 within the right hemisphere across individuals (Weiner et al., 2014; Fig. 5B). On the contrary, a 1 cm disk at the posterior tip of the MFS only defines $48 \pm 9\%$ of pFus-faces/FFA-1 within the right hemisphere across individuals (Fig. 5B). Consequently, the morphological stability of the anterior tip of the MFS compared to the morphological variability of the posterior tip of the MFS (which was described in the first section)

has functional implications in which the anterior tip of the MFS is a landmark predicting the cortical location of a functional region selective for faces. It is important to emphasize that this structural-functional correspondence is not epiphenomenal as electrical stimulation to face-selective regions located lateral to the MFS induces perceptual distortions of faces (Parvizi et al., 2012; Rangarajan et al., 2014). Thus, simply identifying the anterior tip of the MFS not only identifies the location of a functional region implicated in high-level visual processing, but also offers causal insight into face perception.

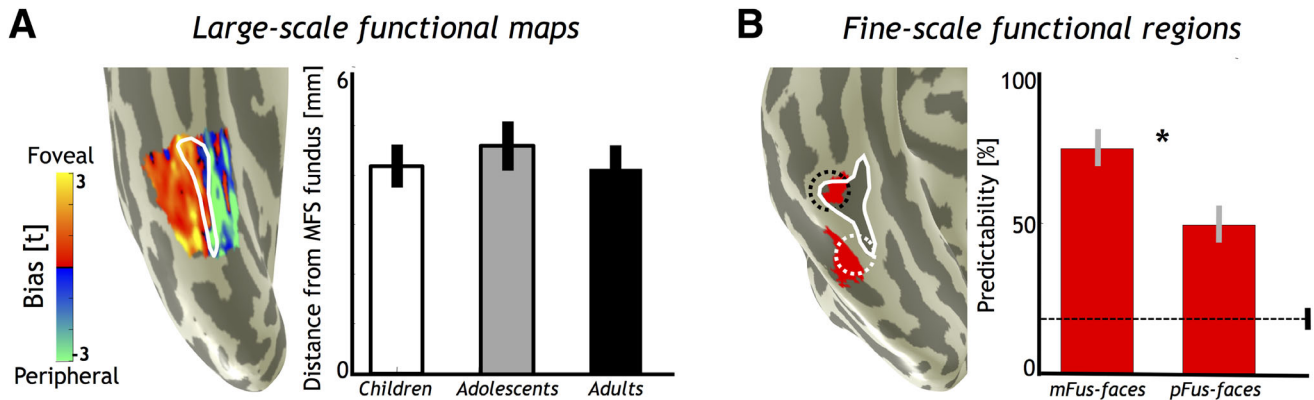


Fig. 5. The MFS identifies transitions in large-scale functional maps and the location of fine-scale functional regions. (A) Left: An example inflated cortical surface reconstruction of an adult right hemisphere zoomed in on ventral occipito-temporal cortex. Colors indicate a map of functional magnetic resonance imaging (fMRI) responses during an experiment in which images were presented in the center of the screen (e.g., foveal) or in the periphery of the screen (e.g., peripheral). A map identifying foveally biased and peripherally-biased cortex was calculated by statistically comparing fMRI responses to foveally and peripherally presented stimuli within each functional voxel in ventral occipito-temporal cortex within children, adolescents, and adults ($N = 12$, each group). As illustrated in this example adult, the functional transition within this eccentricity bias map occurs within the MFS (white) in which pieces of cortex that illustrate preferential responses for processing stimuli presented foveally are lateral to the MFS and those that illustrate preferential responses for processing stimuli that are presented peripherally are medial to the MFS. Right: Average distance between the MFS fundus (in millimeters) and the functional transition within the eccentricity bias map averaged across subjects and hemispheres. The topological layout of the map relative to the MFS was consistent across age groups in which the functional transition was 4.1–4.6 mm from the fundus across age groups. Modified from Weiner et al. (2014). (B) Left: Inflated cortical surface of the right hemisphere from one example adult participant. Red illustrates regions on the FG that illustrate higher fMRI responses to images of faces compared to images of non-face categories. The anterior region is referred to as mFus-faces/FFA-2 and the posterior region is referred to as pFus-faces/FFA-1. To quantify the ability of the MFS to predict the location of these two regions, anatomical disks that were 1 cm in diameter were positioned at the anterolateral (dotted black) or posterolateral (dotted white) tip of the MFS extending to the lateral FG. The overlap between these disks and each functional region was then quantified in each participant included in the experiment (14 adults). Right: Proportion of each face-selective region in the right hemisphere that overlapped with the anatomical disks. There is a stronger structural–functional coupling between the anterior tip of the MFS and mFus-faces/FFA-2 than the posterior tip of the MFS and pFus-faces/FFA-1, which is consistent with the morphological stability and variability of the MFS illustrated in Figure 1 and described in the main text. Dashed line: Proportion of face-selective voxels that are contained within disks centered on stereotaxic coordinates of mFus-faces and pFus-faces published in the literature. *right > left, $P < 0.03$. Modified from Weiner et al. (2014).

The Relationship between Anatomical Connectivity and the MFS

Diffusion MRI (dMRI) and tractography algorithms enable the examination of white matter tracts in the living human brain (Mori and van Zijl, 2002; Catani et al., 2003; Catani and Thiebaut de Schotten, 2008; Tournier et al., 2012; Sotiropoulos et al., 2013; Pestilli et al., 2014; Takemura et al., 2016; Wandell, 2016; Maier-Hein et al., 2017; Yeatman et al., 2018; and many others). Using these methods, findings from recent studies have revealed an elegant correspondence between white matter association fibers and the MFS.

Specifically, recent dMRI studies have identified a consistent topological relationship between the MFS and both vertical and longitudinal white matter tracts. For example, examining the cortical endpoint terminations of the vertical occipital fasciculus (VOF) and the posterior arcuate fasciculus (pAF) relative to cortical folding revealed that the anterior boundary of the VOF and the posterior boundary of the pAF are located near the midpoint of the MFS (Fig. 6A; Yeatman et al., 2014; Weiner et al., 2017b). To link to previous sections of the present article that discussed cytoarchitectonic areas within the FG, the VOF largely terminates posterior to FG3 and FG4 within FG1 and FG2 and surrounding areas (at least at the group level as illustrated in Fig. 6A). In terms of longitudinal tracts, Gomez et al. (2015) identified white

matter fascicles that intersected with functional regions selective for either faces or places in ventral occipito-temporal cortex. These tracts were (a) oriented longitudinally, (b) located below the inferior longitudinal fasciculus, and (c) surrounded the MFS in which face-selective fascicles were positioned lateral to the MFS and place-selective fascicles medial to the MFS (Fig. 6B). These vertical and longitudinal white matter tracts likely contributed to a recent data-driven parcellation of the FG based on connectivity, which delineated three distinct areas that also had a consistent topological relationship relative to the MFS (Zhang et al., 2016). Future seed-based analyses may provide additional clarity regarding the similarity and differences in whole brain connectomes when positioning different seeds on either side of the MFS.

It should also be stated that in addition to non-invasive dMRI and tractography, many invasive methods are used to examine white matter and connectivity in post-mortem human brains such as the Klingler technique (Klingler, 1935), fiber dissections (Curran, 1909), and the Nauta method (Clarke and Miklossey, 1990; Clarke, 1994), among others. To my knowledge, no study has yet examined connectivity relative to the MFS in post-mortem human brains. To fill this gap in knowledge, it would be ideal if one could draw insights from the long history of anatomical tracer studies in macaques. However, as stated in a previous section of the present manuscript, the FG is a hominoid-specific structure and is not present

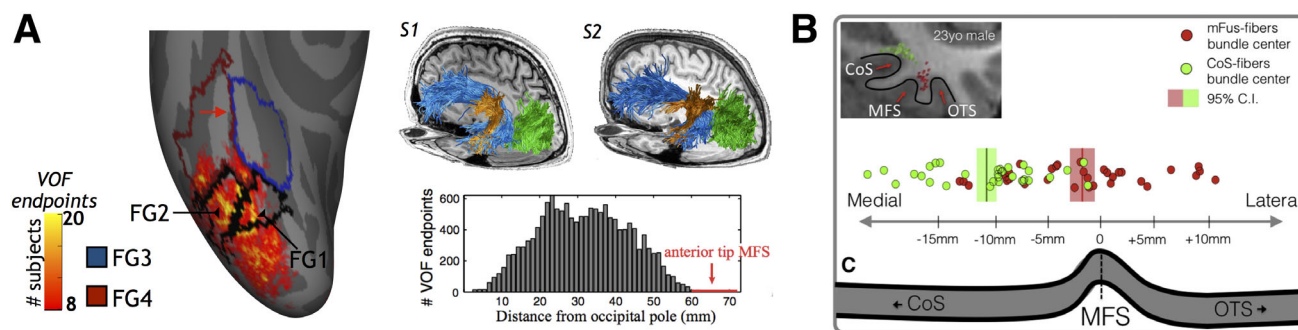


Fig. 6. A consistent relationship between the MFS and the topological positioning of endpoints from vertical and longitudinal white matter tracts. (A) A cortical endpoint map of the vertical occipital fasciculus (VOF) defined from 37 subjects. Cortex-based alignment was used to transform each individual's endpoint map to the FreeSurfer average template (www.freesurfer.net). Cortical surface vertices with consistent, intersubject overlap are shown. The map is thresholded to show the terminations that are common for at least eight subjects. Note that the VOF terminates largely posterior to FG3 (dark blue) and FG4 (maroon) within FG1 and FG2 (black), as well as surrounding areas (at least at the group level). Red arrow indicates the anterior tip of the MFS. Adapted from Weiner et al. (2017b) and Yeatman et al. (2014). Upper right: To anchor the reader as to how the endpoint map was defined, two example subjects (of the 37) are shown with the algorithmically-defined VOF (green) relative to the posterior arcuate (gold) and arcuate fasciculi (blue). Adapted from Weiner et al. (2017b). Bottom right: A histogram showing the distance of each fiber's ventral termination from the occipital pole in stereotaxic coordinates (for all subjects). The VOF rarely extends as far anterior as the anterior tip of the MFS (red arrow shows the mean stereotaxic coordinate and SD across subjects). Modified from Yeatman et al. (2014). (B) In addition to defining white matter tracts algorithmically as in (A), white matter tracts can also be defined by intersecting white matter connectomes with functional regions. For example, a recent study (Gomez et al., 2015) identified separate longitudinal tracts that intersect with face- (red) or place-selective regions (green). Top left: A coronal slice of a typical participant depicting the topology of the CoS, MFS, and occipitotemporal sulcus (OTS) anatomically. Green ("CoS-fibers" in the legend) and red ("mFus-fibers" in the legend) dots illustrate endpoints of place- and face-selective fibers, respectively. Bottom: Center of mFus- (red) and CoS-fibers (green) relative to the fundus of the MFS. Each point is a subject. Face-selective fibers are located lateral to the MFS, while place-selective fibers are located medial to the MFS. Modified from Gomez et al. (2015).

in macaques (Zeki and Marini, 1998; Nasr et al., 2011; Weiner and Zilles, 2016). Thus, relating findings from the plethora of anatomical connectivity studies in macaques to glean insights specifically regarding connectivity of the MFS in humans is impossible since macaques also do not have an MFS. Consequently, future studies, perhaps using new methods to measure fine-scale connections in post-mortem human brains such as polarized light imaging (Caspers et al., 2015b), could further examine the similarity and differences in the connectivity on either side of the MFS. Taken together, the MFS is a landmark linking cytoarchitectonic transitions, functional representations, and white matter fascicles within human ventral occipito-temporal cortex.

The MFS Opens New Questions about the Evolution of Ventral Occipito-Temporal Cortex

While other non-human hominoids such as chimpanzees have an FG (Retzius, 1906; Parr et al., 2009; Chance et al., 2013), it is presently unknown if non-human hominoids also have an MFS. Thus, future morphological studies of the MFS in non-human hominoids will reveal if the MFS is present in both humans and non-human hominoids. This has important implications for understanding the evolution of ventral occipito-temporal cortex: if the MFS is also present in non-human hominoids, then it is a hominoid-specific structure; if it is not, then it is a human-specific structure. Either conclusion motivates understanding how the structure of the FG evolved its many specialized roles—such as face processing and reading—and also, how the large-scale maps and fine-scale clusters that are spatially laid out in an orderly

fashion relative to the MFS contribute to those specialized roles.

Accurate Identification of the MFS Has Translational Applications

The fact that the MFS is an anatomical and functional landmark across spatial scales offers many opportunities for translational applications. For example, in a study comparing the cytoarchitecture of the FG between autistic patients and controls, van Kooten et al. (2008) were unable to relate their findings to functional regions. The authors write:

"The fusiform face area (FFA) within the FG could not be identified separately because neither gross anatomical landmarks nor cytoarchitectonic criteria have been established in the literature to identify the FFA within the FG in human post-mortem brains." van Kooten et al., 2008, p. 989

The recent findings that the MFS is a functional and cytoarchitectonic landmark solves both of these issues. Functionally, a position relative to the MFS in post-mortem tissue can be related either to (1) large-scale functional maps since cortical locations lateral to the MFS are functionally distinct from cortical locations medial to the MFS and (2) to fine-scale functional regions since the anterior tip of the MFS predicts the location of a face-selective region (mFus-faces/FFA-2). Cytoarchitectonically, as the MFS predicts cytoarchitectonic transitions among four different areas, future studies can also use the cytoarchitectonic structure of areas FG1-4 as a

baseline from which to assess typicality in different patient populations (Uppal et al., 2014).

The translational applications do not stop with post-mortem assessments of cytoarchitectonics. Indeed, future studies comparing the structural–functional organization of the brain in controls and patients with disorders that have been associated with the FG could quantify and compare (1) MFS morphology, (2) similarities and differences in the structural–functional coupling among the MFS, large-scale functional maps, and fine-scale functional regions, as well as (3) similarities and differences in the tripartite relationship among the MFS, white matter tracts, and functional regions. Regarding the latter, the study conducted by Gomez et al., (2015) that was mentioned in Section 5 (*The relationship between anatomical connectivity and the MFS*) and depicted in Figure 6B, also quantified similarities and differences between control participants and patients who could not perceive faces (Gomez et al., 2015). Both the controls and the patients had a similar topology of these tracts relative to cortical folding. However, white matter properties within the tracts lateral, but not medial, to the MFS that intersected with face-selective regions were different between the patients compared to controls. Thus, the large-scale topology of the tracts developed normally in the patients, but the tracts were functioning differently in the patients compared to controls. Of course, there are many more examples that one could give, but these examples already show some translational applications that acknowledging the MFS can serve.

Situating the MFS Relative to the Terms Accepted by the TNA

In the *TNA* (FIPAT, 2017; Ten Donkelaar et al., 2017, 2018), the approved label of the fourth temporal gyrus in the “US English” and “UK English” columns is *fusiform gyrus* (p. 64). In the “other” column of the *TNA* for this gyrus, the approved label is *lateral occipitotemporal gyrus* (or LOTG). These two terms date back to the original labeling of the FG by Huschke (1854) and a re-labeling of this macroanatomical structure to the LOTG by Pansch (1866) (see Weiner and Zilles, 2016 for review). Perhaps it is obvious to the reader that the MFS label fits more appropriately with the FG label as opposed to the LOTG label. For example, consider the following two macroanatomical definitions of the MFS: (1) the MFS is a longitudinal sulcus that divides the lateral FG from the medial FG, or (2) the MFS is a longitudinal sulcus that divides the lateral lateral occipito-temporal gyrus from the medial lateral occipito-temporal gyrus. The former is clearer than the latter. One could argue that should the MFS be accepted as the “US English” and “UK English” columns in future revisions of the *TNA*, then *occipitotemporal sulcus* or *lateral occipitotemporal sulcus* could be accepted in the “other” column. However, this would add confusion rather than clarity for two reasons. First, the *TNA* already acknowledges an *occipitotemporal sulcus* or *lateral occipitotemporal sulcus* that is not within the FG (FIPAT, 2017, p. 64), but forms the lateral boundary of the FG. Second, the OTS is morphologically distinct based on its depth compared to the MFS as discussed in the first section of this article (Fig. 1).

Thus, if the goal of the *TNA* is to prevent confusion, I suggest that (a) MFS is the least confusing label for this

sulcus for the “US English” and “UK English” columns of the *TNA* table because it is already widely used in the neuroscience literature (Retzius, 1896; Bailey and von Bonin, 1951; Puce et al., 1996; Nobre et al., 1998; Allison et al., 1999; Weiner and Grill-Spector 2010, 2013; Nasr et al., 2011; Petrides 2012; Grill-Spector and Weiner, 2014; McGugin et al., 2014; Weiner et al., 2014; Yeatman et al., 2014; Gomez et al., 2015; McGugin et al., 2015; Lorenz et al., 2017; van den Hurk et al., 2015; Jacques et al., 2016; Kadipasaoglu et al., 2016; Natu et al., 2016; Weiner and Zilles 2016; Gomez et al., 2017; Weiner et al., 2017a) and (b) *sulcus sagittalis gyri fusiformis* (as originally proposed by Retzius (1896)) is the least confusing for the “other” column of the *TNA* table because it is also historically accurate and clearly differentiable from other sulcal names accepted by the *TNA*. Concomitantly, MFS and *sulcus sagittalis gyri fusiformis* seem to be the labels that will minimize confusion and maximize clarity among neuroanatomists spanning basic and applied research, as well as those in different medical fields.

CONCLUSIONS

The MFS (*sulcus sagittalis gyri fusiformis*) has been identified by the eyes of expert neuroanatomists since 1896 and by algorithms over 120 years later. And yet, the MFS is more than just identifiable in every hemisphere. It is also a landmark that identifies (a) cytoarchitectonic transitions among four different areas, (b) transitions among a multitude of large-scale functional maps, (c) the location of a fine-scale functional region that is causally implicated in visual perception, and (d) the cortical location of endpoints from vertical and longitudinal white matter fascicles. Altogether, this article serves as a comprehensive reference source regarding these anatomical and functional details of the MFS, as well as provides a growing number of reasons to include the MFS as a recognized neuroanatomical structure in future revisions of the *TNA*. Formal acknowledgement of the MFS by the *TNA* has benefits not only for basic research in neuroanatomy and neuroscience, but also for translational applications that could use the MFS for both potential diagnostic purposes as well as for improved understanding of structural–functional organization of the FG in health and disease across spatial scales—from cellular to areal and systems organization.

ACKNOWLEDGMENTS

This work was supported by start-up funds provided by the University of California, Berkeley and the Helen Wills Neuroscience Institute. I thank all of my collaborators who have contributed to the studies that are comprehensively reviewed in this article, especially Kalanit Grill-Spector, Karl Zilles, and Katrin Amunts.

LITERATURE CITED

- Ahrens P, Schleicher A, Zilles K, Werner L. 1990. Image analysis of nissl-stained neuronal perikarya in the primary visual cortex of the rat: Automatic detection and segmentation of neuronal profiles with nuclei and nucleoli. *J Microsc* 157(Pt 3):349–365.
- Allison T, Puce A, Spencer DD, McCarthy G. 1999. Electrophysiological studies of human face perception. I: Potentials generated in

- occipitotemporal cortex by face and non-face stimuli. *Cereb Cortex* 9(5):415–430.
- Amunts K, Zilles K. 2015. Architectonic mapping of the human brain beyond Brodmann. *Neuron* 88(6):1086–1107.
- Amunts K, Istomin V, Schleicher A, Zilles K. 1995. Postnatal development of the human primary motor cortex: A quantitative cytoarchitectonic analysis. *Anat Embryol (Berl)* 192(6):557–571.
- Bailey P, von Bonin G. 1951. *The isocortex of man*. Urbana: University of Illinois Press.
- Bouhali F, Thiebaut de Schotten M, Pinel P, Poupon C, Mangin JF, Dehaene S, Cohen L. 2014. Anatomical connections of the visual word form area. *J Neurosci* 34(46):15402–15414.
- Brodmann K. 1909. *Vergleichende lokalisationslehre der groÙhirnrinde in ihren prinzipien dargestellt auf grund des zellbaues*. Leipzig: Johann Ambrosius Barth Verlag.
- Caspers J. 2013. *Structural and functional characterization of object-related regions in the human visual cortex C and O*. Düsseldorf: Vogt Institute for Brain Research, Heinrich-Heine University.
- Caspers J, Zilles K, Eickhoff SB, Schleicher A, Mohlberg H, Amunts K. 2013. Cytoarchitectonical analysis and probabilistic mapping of two extrastriate areas of the human posterior fusiform gyrus. *Brain Struct Funct* 218(2):511–526.
- Caspers J, Palomero-Gallagher N, Caspers S, Schleicher A, Amunts K, Zilles K. 2015a. Receptor architecture of visual areas in the face and word-form recognition region of the posterior fusiform gyrus. *Brain Struct Funct* 220(1):205–219.
- Caspers S, Axer M, Caspers J, Jockwitz C, Jutten K, Reckfort J, Grassel D, Amunts K, Zilles K. 2015b. Target sites for transcallosal fibers in human visual cortex – A combined polarized light imaging study. *Cortex* 72:40–53.
- Catani M, Thiebaut de Schotten M. 2008. A diffusion tensor imaging tractography atlas for virtual in vivo dissections. *Cortex* 44(8):1105–1132.
- Catani M, Jones DK, Donato R, Ffytche DH. 2003. Occipito-temporal connections in the human brain. *Brain* 126(Pt 9):2093–2107.
- Chance SA, Sawyer EK, Clover LM, Wicinski B, Hof PR, Crow TJ. 2013. Hemispheric asymmetry in the fusiform gyrus distinguishes *Homo sapiens* from chimpanzees. *Brain Struct Funct* 218(6):1391–1405.
- Clarke S. 1994. Association and intrinsic connections of human extrastriate visual cortex. *Proc Biol Sci* 257(1348):87–92.
- Clarke S, Miklossey J. 1990. Occipital cortex in man: Organization of callosal connections, related myelo- and cytoarchitecture, and putative boundaries of functional areas. *J Comp Neurol* 298(2):188–214.
- Cohen L, Dehaene S, Naccache L, Lehericy S, Dehaene-Lambertz G, Henaff MA, Michel F. 2000. The visual word form area: Spatial and temporal characterization of an initial stage of reading in normal subjects and posterior split-brain patients. *Brain* 123(Pt 2):291–307.
- Connolly JC. 1950. *External morphology of the primate brain*. Springfield: C. C. Thomas.
- Curran EJ. 1909. A new association fiber tract in the cerebrum. With remarks on the fiber tract dissection method of studying the brain. *J Comp Neurol Psychol* 19:645–656.
- Dale AM, Fischl B, Sereno MI. 1999. Cortical surface-based analysis. I Segmentation and surface reconstruction. *Neuroimage* 9(2):179–194.
- Damasio AR, Damasio H, Van Hoesen GW. 1982. Prosopagnosia: Anatomic basis and behavioral mechanisms. *Neurology* 32(4):331–341.
- Economo C, Koskinas G. 1925. *Die cytoarchitektonik der hirnrinde des erwachsenen menschen*. Berlin: Springer.
- Farah MJ. 1990. *Visual agnosia: Disorders of object recognition and what they tell us about normal vision*. Cambridge, MA: MIT Press.
- FIPAT. 2017. Terminologica neuroanatomica. February 2017 ed. FIPAT.librarydal.ca: Federative International Programme for Anatomical Terminology. p. 1–84.
- Fischl B, Sereno MI, Tootell RB, Dale AM. 1999. High-resolution intersubject averaging and a coordinate system for the cortical surface. *Hum Brain Mapp* 8(4):272–284.
- Gauthier I, Tarr MJ. 2016. Visual object recognition: Do we (finally) know more now than we did? *Annu Rev Vis Sci* 2:377–396.
- Gauthier I, Tarr MJ, Anderson AW, Skudlarski P, Gore JC. 1999. Activation of the middle fusiform ‘face area’ increases with expertise in recognizing novel objects. *Nat Neurosci* 2(6):568–573.
- Gauthier I, Skudlarski P, Gore JC, Anderson AW. 2000. Expertise for cars and birds recruits brain areas involved in face recognition. *Nat Neurosci* 3(2):191–197.
- Glezer LS, Riesenhuber M. 2013. Individual variability in location impacts orthographic selectivity in the “visual word form area”. *J Neurosci* 33(27):11221–11226.
- Gomez J, Pestilli F, Witthoft N, Golarai G, Liberman A, Poltoratski S, Yoon J, Grill-Spector K. 2015. Functionally defined white matter reveals segregated pathways in human ventral temporal cortex associated with category-specific processing. *Neuron* 85(1):216–227.
- Gomez J, Barnett MA, Natu V, Mezer A, Palomero-Gallagher N, Weiner KS, Amunts K, Zilles K, Grill-Spector K. 2017. Microstructural proliferation in human cortex is coupled with the development of face processing. *Science* 355(6320):68–71.
- Grill-Spector K. 2003. The neural basis of object perception. *Curr Opin Neurobiol* 13(2):159–166.
- Grill-Spector K, Weiner KS. 2014. The functional architecture of the ventral temporal cortex and its role in categorization. *Nat Rev Neurosci* 15(8):536–548.
- Grill-Spector K, Knouf N, Kanwisher N. 2004. The fusiform face area subserves face perception, not generic within-category identification. *Nat Neurosci* 7(5):555–562.
- Haxby JV, Horowitz B, Ungerleider LG, Maisog JM, Pietrini P, Grady CL. 1994. The functional organization of human extrastriate cortex: A pet-rctb study of selective attention to faces and locations. *J Neurosci* 14(11 Pt 1):6336–6353.
- Haxby JV, Guntupalli JS, Connolly AC, Halchenko YO, Conroy BR, Gobbini MI, Hanke M, Ramadge PJ. 2011. A common, high-dimensional model of the representational space in human ventral temporal cortex. *Neuron* 72(2):404–416.
- Huschke E. 1854. *Schaedel, hirn und seele des menschen und der thiere nach alter, geschlecht und race, dargestellt nach neuen methoden und untersuchungen*. Jena: Mauke.
- Huth AG, Nishimoto S, Vu AT, Gallant JL. 2012. A continuous semantic space describes the representation of thousands of object and action categories across the human brain. *Neuron* 76(6):1210–1224.
- Istomin V, Amunts K. 1992. Application of mathematical morphology algorithms for automatic quantification of the cytoarchitecture of human neocortex. *Vis Voice Magazine* 6:142–153.
- Istomin VV, Shklyarov MI. 1984. Automated investigation of the human cerebral cortex with a tv-based image analyse system (russ.). *Zhurnal Nevropatologii i Psikhiatrii imeni SSKorsakova* 7:969–974.
- Jacques C, Witthoft N, Weiner KS, Foster BL, Rangarajan V, Hermes D, Miller KJ, Parvizi J, Grill-Spector K. 2016. Corresponding ecog and fmri category-selective signals in human ventral temporal cortex. *Neuropsychologia* 83:14–28.
- Jonas J, Jacques C, Liu-Shuang J, Brissart H, Colnat-Coulbois S, Maillard L, Rossion B. 2016. A face-selective ventral occipitotemporal map of the human brain with intracerebral potentials. *Proc Natl Acad Sci U S A* 113(28):E4088–E4097.
- Kadipasaoglu CM, Conner CR, Whaley ML, Baboyan VG, Tandon N. 2016. Category-selectivity in human visual cortex follows cortical topology: A grouped iceeg study. *PLoS One* 11(6):e0157109.
- Kanwisher N, McDermott J, Chun MM. 1997. The fusiform face area: A module in human extrastriate cortex specialized for face perception. *J Neurosci* 17(11):4302–4311.
- Klingler J. 1935. Erleichterung der makroskopischen Präparation des Gehirns durch den Gefrierprozess. *Schweiz Arch Neurol Psychiatr* 36:247e256.
- Konen CS, Behrmann M, Nishimura M, Kastner S. 2011. The functional neuroanatomy of object agnosia: A case study. *Neuron* 71(1):49–60.
- Konkle T, Oliva A. 2012. A real-world size organization of object responses in occipitotemporal cortex. *Neuron* 74(6):1114–1124.
- Lorenz S, Weiner KS, Caspers J, Mohlberg H, Schleicher A, Bludau S, Eickhoff S, Grill-Spector K, Zilles K, Amunts K. 2017. Two new cytoarchitectonic areas on the human mid-fusiform gyrus. *Cereb Cortex* 27(1):373–385.

- Maier-Hein KH, Neher PF, Houde JC, Cote MA, Garyfallidis E, Zhong J, Chamberland M, Yeh FC, Lin YC, Ji Q, et al. 2017. The challenge of mapping the human connectome based on diffusion tractography. *Nat Commun* 8(1):1349.
- Malach R, Reppas JB, Benson RR, Kwong KK, Jiang H, Kennedy WA, Ledden PJ, Brady TJ, Rosen BR, Tootell RB. 1995. Object-related activity revealed by functional magnetic resonance imaging in human occipital cortex. *Proc Natl Acad Sci U S A* 92(18):8135–8139.
- Malach R, Levy I, Hasson U. 2002. The topography of high-order human object areas. *Trends Cogn Sci* 6(4):176–184.
- Martin A. 2007. The representation of object concepts in the brain. *Annu Rev Psychol* 58:25–45.
- McGugin RW, Newton AT, Gore JC, Gauthier I. 2014. Robust expertise effects in right ffa. *Neuropsychologia* 63:135–144.
- McGugin RW, Van Gulick AE, Tamber-Rosenau BJ, Ross DA, Gauthier I. 2015. Expertise effects in face-selective areas are robust to clutter and diverted attention, but not to competition. *Cereb Cortex* 25:2610–2622.
- Mickle WJ. 1897. Atypical and unusual brain-forms, especially in relation to mental status: A study on brain-surface morphology XLIII (180):1–32.
- Mori S, van Zijl PC. 2002. Fiber tracking: principles and strategies—a technical review. *NMR Biomed* 15:468–480.
- Nasr S, Liu N, Devaney KJ, Yue X, Rajimehr R, Ungerleider LG, Tootell RB. 2011. Scene-selective cortical regions in human and nonhuman primates. *J Neurosci* 31(39):13771–13785.
- Natu VS, Barnett MA, Hartley J, Gomez J, Stigliani A, Grill-Spector K. 2016. Development of neural sensitivity to face identity correlates with perceptual discriminability. *J Neurosci* 36(42):10893–10907.
- Nobre AC, Allison T, McCarthy G. 1998. Modulation of human extrastriate visual processing by selective attention to colours and words. *Brain* 121(Pt 7):1357–1368.
- Pansch A. 1866. *De sulcis et gyris in cerebris: Simiarum et hominum*. Mohr: Kiliae.
- Parr LA, Hecht E, Barks SK, Preuss TM, Votaw JR. 2009. Face processing in the chimpanzee brain. *Curr Biol* 19(1):50–53.
- Parvizi J, Jacques C, Foster BL, Withoft N, Rangarajan V, Weiner KS, Grill-Spector K. 2012. Electrical stimulation of human fusiform face-selective regions distorts face perception. *J Neurosci* 32(43):14915–14920.
- Pestilli F, Yeatman JD, Rokem A, Kay KN, Wandell BA. 2014. Evaluation and statistical inference for human connectomes. *Nat Methods* 11:1058–1063.
- Petrides M. 2012. *The human cerebral cortex*. New York: Academic Press.
- Puce A, Allison T, Gore JC, McCarthy G. 1995. Face-sensitive regions in human extrastriate cortex studied by functional MRI. *J Neurophysiol* 74(3):1192–1199.
- Puce A, Allison T, Asgari M, Gore JC, McCarthy G. 1996. Differential sensitivity of human visual cortex to faces, letterstrings, and textures: A functional magnetic resonance imaging study. *J Neurosci* 16(16):5205–5215.
- Puce A, Allison T, McCarthy G. 1999. Electrophysiological studies of human face perception. Iii: Effects of top-down processing on face-specific potentials. *Cereb Cortex* 9(5):445–458.
- Rangarajan V, Hermes D, Foster BL, Weiner KS, Jacques C, Grill-Spector K, Parvizi J. 2014. Electrical stimulation of the left and right human fusiform gyrus causes different effects in conscious face perception. *J Neurosci* 34:12828–12836.
- Rauch F, Schleicher A, Zilles K. 1989. Recognition of the retrograde reaction in motoneurons using an image analysing system. *J Neurosci Methods* 30(3):255–262.
- Retzius G. 1896. *Das menschenhirn. Studien in der makroskopischen morphologie*. Stockholm: Kgl. Buchdr. P. A. Norstedt and Söner.
- Retzius G. 1906. *Cerebra simiarum illustrata. Das affenhirn in bildlicher darstellung*. Stockholm: G. Fischer.
- Rosenke M, Weiner KS, Barnett MA, Zilles K, Amunts K, Goebel R, Grill-Spector K. 2018. A cross-validated cytoarchitectonic atlas of the human ventral visual stream. *Neuroimage* 170:257–270.
- Rossion B. 2008. Constraining the cortical face network by neuroimaging studies of acquired prosopagnosia. *Neuroimage* 40(2):423–426.
- Rossion B, Caldara R, Seghier M, Schuller AM, Lazeyras F, Mayer E. 2003. A network of occipito-temporal face-sensitive areas besides the right middle fusiform gyrus is necessary for normal face processing. *Brain* 126(Pt 11):2381–2395.
- Rossion B, Jacques C, Jonas J. 2018. Mapping face categorization in the human ventral occipitotemporal cortex with direct neural intracranial recordings. *Ann N Y Acad Sci* 1426:5–24.
- Schlaug G, Schleicher A, Zilles K. 1995. Quantitative analysis of the columnar arrangement of neurons in the human cingulate cortex. *J Comp Neurol* 351(3):441–452.
- Schleicher A, Zilles K. 1990. A quantitative approach to cytoarchitectonics: Analysis of structural inhomogeneities in nervous tissue using an image analyser. *J Microsc* 157(Pt 3):367–381.
- Schleicher A, Zilles K, Wree A. 1986. A quantitative approach to cytoarchitectonics: Software and hardware aspects of a system for the evaluation and analysis of structural inhomogeneities in nervous tissue. *J Neurosci Methods* 18(1–2):221–235.
- Schleicher A, Amunts K, Geyer S, Morosan P, Zilles K. 1999. Observer-independent method for microstructural parcellation of cerebral cortex: A quantitative approach to cytoarchitectonics. *Neuroimage* 9(1):165–177.
- Schleicher A, Palomero-Gallagher N, Morosan P, Eickhoff SB, Kowalski T, de Vos K, Amunts K, Zilles K. 2005. Quantitative architectural analysis: A new approach to cortical mapping. *Anat Embryol (Berl)*. 210(5–6):373–386.
- Scholtens LH, de Reus MA, de Lange SC, Schmidt R, van den Heuvel MP. 2018. An MRI von Economo – Koskinas atlas. *Neuroimage* 170:249–256.
- Sergent J, Ohta S, MacDonald B. 1992. Functional neuroanatomy of face and object processing. A positron emission tomography study. *Brain* 115(Pt 1):15–36.
- Serra J. 1986. Mathematical morphology. *Comput Vis Graphics Image Process* 35:283–305.
- Smith GE. 1907. A new topographical survey of the human cerebral cortex, being an account of the distribution of the anatomically distinct cortical areas and their relationship to the cerebral sulci. *J Anat Physiol* 41(Pt 4):237–254.
- Sotiropoulos SN, Jbabdi S, Xu J, Andersson JL, Moeller S, Auerbach EJ, Glasser MF, Hernandez M, Sapiro G, Jenkinson M, et al. 2013. Advances in diffusion MRI acquisition and processing in the human connectome project. *Neuroimage* 80:125–143.
- Takemura H, Rokem A, Winawer J, Yeatman JD, Wandell BA, Pestilli F. 2016. A major human white matter pathway between dorsal and ventral visual cortex. *Cereb Cortex* 26(5):2205–2214.
- Ten Donkelaar HJ, Broman J, Neumann PE, Puelles L, Riva A, Tubbs RS, Kachlik D. 2017. Towards a terminologia neuroanatomica. *Clin Anat* 30(2):145–155.
- Ten Donkelaar HJ, Kachlik D, Tubbs RS. 2018. *An Illustrated Terminologia Neuroanatomica: A concise encyclopedia of human neuroanatomy*. Switzerland: Springer.
- Tournier JD, Calamante F, Connelly A. 2012. MRtrix: diffusion tractography in crossing fiber regions. *Int J Imaging Syst Technol* 22: 53–66.
- Uppal N, Gianatiempo I, Wicinski B, Schmeidler J, Heinsen H, Schmitz C, Buxbaum JD, Hof PR. 2014. Neuropathology of the posterior inferior occipitotemporal gyrus in children with autism. *Mol Autism* 5(1):17.
- van den Hurk J, Pegado F, Martens F, Op de Beeck HP. 2015. The search for the face of the visual homunculus. *Trends Cogn Sci* 19(11):638–641.
- Van Essen DC. 2005. A population-average, landmark- and surface-based (pals) atlas of human cerebral cortex. *Neuroimage* 28(3):635–662.
- van Kooten IA, Palmén SJ, von Cappeln P, Steinbusch HW, Korr H, Heinsen H, Hof PR, van Engeland H, Schmitz C. 2008. Neurons in the fusiform gyrus are fewer and smaller in autism. *Brain* 131(Pt 4):987–999.
- Vogt O. 1904. *Neurobiologische arbeiten*. Jena: Verlag von Gustav Fischer.
- Wandell BA. 2016. Clarifying human white matter. *Annu Rev Neurosci* 39:103–128.
- Wandell BA, Rauschecker AM, Yeatman JD. 2012. Learning to see words. *Annu Rev Psychol* 63:31–53.

- Weiner KS, Grill-Spector K. 2010. Sparsely-distributed organization of face and limb activations in human ventral temporal cortex. *Neuroimage* 52(4):1559–1573.
- Weiner KS, Grill-Spector K. 2013. Neural representations of faces and limbs neighbor in human high-level visual cortex: Evidence for a new organization principle. *Psychol Res* 77(1):74–97.
- Weiner KS, Zilles K. 2016. The anatomical and functional specialization of the fusiform gyrus. *Neuropsychologia* 83:48–62.
- Weiner KS, Sayres R, Vinberg J, Grill-Spector K. 2010. Fmri-adaptation and category selectivity in human ventral temporal cortex: Regional differences across time scales. *J Neurophysiol* 103(6):3349–3365.
- Weiner KS, Golarai G, Caspers J, Chuapoco MR, Mohlberg H, Zilles K, Amunts K, Grill-Spector K. 2014. The mid-fusiform sulcus: A landmark identifying both cytoarchitectonic and functional divisions of human ventral temporal cortex. *Neuroimage* 84:453–465.
- Weiner KS, Barnett MA, Lorenz S, Caspers J, Stigliani A, Amunts K, Zilles K, Fischl B, Grill-Spector K. 2017a. The cytoarchitecture of domain-specific regions in human high-level visual cortex. *Cereb Cortex* 27(1):146–161.
- Weiner KS, Yeatman JD, Wandell BA. 2017b. The posterior arcuate fasciculus and the vertical occipital fasciculus. *Cortex* 97:274–276.
- Weiner KS, Natu VS, Grill-Spector K. 2018. On object selectivity and the anatomy of the human fusiform gyrus. *Neuroimage* 173:604–609.
- Wree A, Schleicher A, Zilles K. 1982. Estimation of volume fractions in nervous tissue with an image analyzer. *J Neurosci Methods* 6(1–2):29–43.
- Yeatman JD, Weiner KS, Pestilli F, Rokem A, Mezer A, Wandell BA. 2014. The vertical occipital fasciculus: A century of controversy resolved by in vivo measurements. *Proc Natl Acad Sci U S A* 111:E5214–E5223.
- Yeatman JD, Richie-Halford A, Smith JK, Keshavan A, Rokem A. 2018. A browser-based tool for visualization and analysis of diffusion mri data. *Nat Commun* 9(1):940.
- Zeki S, Marini L. 1998. Three cortical stages of colour processing in the human brain. *Brain* 121(9):1669–1685.
- Zhang W, Wang J, Fan L, Zhang Y, Fox PT, Eickhoff SB, Yu C, Jiang T. 2016. Functional organization of the fusiform gyrus revealed with connectivity profiles. *Hum Brain Mapp* 37(8):3003–3016.
- Zilles K. 1978. A quantitative approach to cytoarchitectonics. Ii The allocortex of *Tupaia belangeri*. *Anat Embryol (Berl)* 154(3):335–352.
- Zilles K, Schleicher A, Kretschmann HJ. 1978. Automatic morphometric analysis of retrograde changes in the nucleus n. Facialis at different ontogenetic stages in the rat. *Cell Tissue Res* 190(2):285–299.
- Zilles K, Zilles B, Schleicher A. 1980. A quantitative approach to cytoarchitectonics. Vi The areal pattern of the cortex of the albino rat. *Anat Embryol (Berl)* 159(3):335–360.
- Zilles K, Werners R, Busching U, Schleicher A. 1986. Ontogenesis of the laminar structure in areas 17 and 18 of the human visual cortex. A quantitative study. *Anat Embryol (Berl)* 174(3):339–353.